Singh, J.; Altinakar, M. S.; Ding, Y.

Simulating Shallow Water Flows over Complex Topography Using a Well-Balanced And Positivity Preserving Central Scheme

Proceedings of Ninth International Conference on Hydro-Science and Engineering (ICHE 2010), IIT Madras, Chennai, India.
2 - 5 August 2010

SIMULATING SHALLOW WATER FLOWS OVER COMPLEX TOPOGRAPHY USING A WELL-BALANCED AND POSITIVITY PRESERVING CENTRAL SCHEME

Singh J.[1], M.S. Altinakar[2] and Y. Ding[3]

Abstract: *This paper presents a two-dimensional (2D) numerical model for the simulation of shallow, transient free-surface flows over a natural topography. The governing equations are 2D depth averaged non-linear shallow water equations with source terms due to bottom elevation and non-linear friction terms. The equations are solved using a central upwind scheme (Kurganov and Petrova 2007). The main advantages of this scheme are smaller numerical dissipation, high resolution and ease of implementation. This scheme is well balanced and guarantees the positivity of the depth at wet and dry cell interface over complex topography. For the steady state conditions, the flux terms are exactly balanced by the source terms due to bottom elevation maintaining the lake at rest conditions. The numerical model results are verified using analytical solutions and validated using experimental data from laboratory and model tests as well as field data gathered from past dam break events. Some of the simulated benchmark tests involved a mixture of various flow regimes, i.e. supercritical, sub-critical and transcritical flows. It was observed that the simulated results regarding flood arrival time and time history of flow depth and discharge are in good agreement with the analytical solutions as well as the experimental data from laboratory tests and field observations. The developed numerical model was also used to simulate the Malpasset dam failure event occurred in France in 1959. It is shown that the simulated results agree well with the observed field data and model tests.*

Keywords *Shallow water equations; System of hyperbolic conservation laws; Central upwind scheme; Well balanced schemes; Flood simulation on complex topography.*

INTRODUCTION

The study of water flows is an integral part of many engineering and environmental problems. Free surface water flows are found in nature in many situations such as open channel flows, river flows, coastal flows, tsunamis, dam break flows etc. These flows are characterized by the presence of a free surface and can be modeled using shallow water equations, which form a system of nonlinear hyperbolic equations. In recent years, there has been a substantial research emphasis on the development of numerical models to simulate these flows. For instance, Zhou et al. (2001) provided a good historic revision and features required for 2D river flow simulation

1 Research Scientist, National Center for Computational Hydroscience and Engineering, The University of Mississippi, Oxford, MS, 38655, USA, Email: singh@nche.olemiss.edu
2 Research Professor and Director, National Center for Computational Hydroscience and Engineering, The University of Mississippi, Oxford, MS, 38655, USA, Email: altinakar@ncche.olemiss.edu. [member IAHR]
3 Research Assistant Professor, National Center for Computational Hydroscience and Engineering, The University of Mississippi, Oxford, MS, 38655, USA, Email: ding@ncche.olemiss.edu [member IAHR]

model such as wetting drying front treatment, treatment of bed elevation terms in sources terms, steady and unsteady flow and subcritical or supercritical conditions. Brufau et al. (2004) developed two-dimensional (2D) numerical model to simulate river flows and provided numerically stable and conservative solution. Ying et al. (2003) developed numerical models for flow generated by dam failure or levee breaching process using conservative form of shallow water equations. Caleffi et al. (2002) used finite volume method for modelling the extreme flood events in natural channels. Valiani et al. (2002) modeled Malpasset dam break event using 2D finite volume method.

The depth averaged non-linear shallow water equations govern the free surface shallow flows. These are commonly used to model flood flows in rivers, open channels or hydrodynamics in coastal areas etc. These equations are the member of the general class of equations called hyperbolic conservation laws. This system of equations admits steady-state solutions in which the non-zero flux terms are balanced by the sources terms. These nonlinear hyperbolic equations admit solutions that involve discontinuous and nonlinear waves, such as shocks and rarefactions, as well as wet-dry interfaces. In the case of water flow, shocks correspond to standing or moving hydraulic jumps, which are difficult to capture by simple solution schemes. A variety of high-order well-balanced schemes for the Saint-Venant system of equations can be found in (LeVeque, 1998, Kurganov and Levy, 2002, Russo 2005, Noelle et al. 2006). These schemes produce good approximation of the quasi-steady solutions and non-stationary steady states. The difficulty may occur where dry states are encountered in the solutions domain. In this case, due to numerical oscillations, water depth (h) may become negative and the numerical computation will break down as the wave speeds are computed as eigenvalues ($u + \sqrt{gh}$) of the Jacobian of the Eq. 1. Another difficulty with some of the schemes can be that they can only be applied in case of a continuous bottom topography function.

The model presented in this paper is based on the central upwind scheme (Kuraganov and Petrova 2007) which is simple to implement and robust in computations. The main advantage of this scheme is its capability to simultaneously preserve the positivity of flow depth and stationary steady state solutions of lake at rest case. One dimensional (1D) version of the present model was tested against the analytical solutions of selected benchmark problems (Zhou et al. 2001) and experimental data published in the literature (Brufau et al. 2002). The 2D version of the present model was then applied to a real-life case of dam-break flood simulation. This paper is organized as follows: In section 2, the detailed description of the model development is presented. In section 3, 1D model is validated and the simulations are compared with analytical solution and experimental data. Section 4 presents the application of 2D version of the present model to simulate the Malpasset dam break event.

MODEL DEVELOPMENT

Governing Equations

The 2D shallow water equations describing the free surface flow over a bottom topography that can be defined as a height field, *B(x,y)* can be written as:

$$\begin{bmatrix} h \\ hu \\ hv \end{bmatrix}_t + \begin{bmatrix} hu \\ hu^2 + \frac{1}{2}gh^2 \\ huv \end{bmatrix}_x + \begin{bmatrix} hv \\ huv \\ hv^2 + \frac{1}{2}gh^2 \end{bmatrix}_y = \begin{bmatrix} 0 \\ -gh\frac{\partial B}{\partial x} - S_{fx} \\ -gh\frac{\partial B}{\partial x} - S_{fy} \end{bmatrix} \quad (1)$$

where t is time and x and y are Cartesian coordinates describing the horizontal plane, $h(x,y,t)$ is the depth of the flow, $u(x,y,t)$ and $v(x,y,t)$ are the components of the depth-averaged velocities in x and y directions, respectively. The gravitational acceleration is denoted by g. S_{fx} and S_{fy} are the components of bottom friction term due to its roughness in x and y directions, respectively. The first equation represents the conservation of mass, and the remaining two equations represent the conservation of momentum in x and y directions. The source terms are discretized by paying attention to preserve the steady-state solutions. The water surface elevation is represented by $w(x,y,t)$ such that $w = h+B$ (see figure 1). The $w(x,y,t)$ remains constant for the steady state condition. By doing simple algebraic manipulations, the Eq.1 is written in terms of $w(x,y,t)$. The bottom elevation $B(x)$ remains constant in time.

$$\left\{ \begin{aligned} & w_t + (hu)_x + (hv)_y = 0, \\ & (hu)_t + \left[\frac{(hu)^2}{w-B} + \frac{1}{2}g(w-B)^2 \right]_x + \left[\frac{(hu)(hv)}{w-B} \right]_y = -g(w-B)\frac{\partial B}{\partial x} - S_{fx} \\ & (hv)_t + \left[\frac{(hu)(hv)}{w-B} \right]_x + \left[\frac{(hv)^2}{w-B} + \frac{1}{2}g(w-B)^2 \right]_y = -g(w-B)\frac{\partial B}{\partial y} - S_{fy} \end{aligned} \right\} \quad (2)$$

The bottom frictions terms S_{fx} and S_{fy} in the above equations are described as $S_{fx} = gu\sqrt{u^2+v^2}/C^2(w-B)$ and $S_{fy} = gv\sqrt{u^2+v^2}/C^2(w-B)$, where the C is the Chezy coefficient and is calculated as $C = (w-B)^{1/6}/n$ and n is the Manning's coefficient.

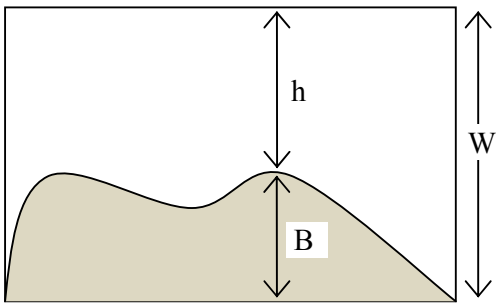

Fig.1 Variables definition sketch

The Eq.2 can be written in vector form as follows:

$$U_t + F(U,B)_x + G(U,B)_y = S(U,B) \quad (3)$$

where U, $F(U,B)$, $G(U,B)$ and $S(U,B)$ are the vector of primitive variables, fluxes in x and y

direction and sources, defined as follows:

$$U = \begin{bmatrix} w \\ hu \\ hv \end{bmatrix}_t , \; F(U,B)_x = \begin{bmatrix} hu \\ \frac{(hu)^2}{w-B} + \frac{1}{2} g(w-B)^2 \\ \frac{(hu)(hv)}{w-B} \end{bmatrix}_x \quad G(U,B)_y = \begin{bmatrix} hv \\ \frac{(hu)(hv)}{w-B} \\ \frac{(hv)^2}{w-B} + \frac{1}{2} g(w-B)^2 \end{bmatrix}_y ,$$

$$S(U,B,) = \begin{bmatrix} 0 \\ -gh \frac{\partial B}{\partial x} - S_{fx} \\ -gh \frac{\partial B}{\partial x} - S_{fy} \end{bmatrix},$$

Numerical Scheme

The discretization of the above equations is based on the finite volume method. The computational domain is a regular Cartesian grid in the horizontal plane as shown in figure 2. The grid is uniform with Δx as its spatial scale. The distance of the cell from the origin is $x_a = a.\Delta x$ and the finite volume of the cells C_{ij} is defined as $\left[x_{i-1/2}, x_{i+1/2}, y_{j-1/2}, y_{j+1/2}\right]$. The locations represented by $x_{i+1/2}$, $x_{i-1/2}$, $y_{j+1/2}$, $y_{j-1/2}$, are designated as the mid-point of sides of the cell volume in both x and y direction. These mid-point locations are superscripted as east (^{E}), west (^{W}), north (^{N}) and south (^{S}) in the equations. The primitive variables are considered at the cell center and the bottom elevation is considered at the four corner of the cell.

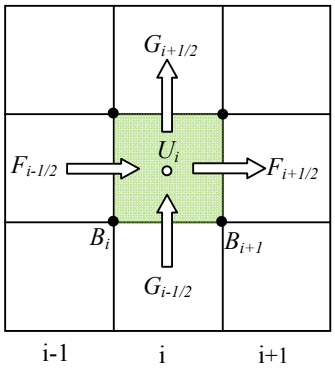

Fig. 2 Computational grid

The central upwind scheme (Kurganov and Petrova 2007) to solve the system of Eq.2 is as follows;

$$\frac{d}{dt} U_{i,j}(t) = -\frac{H^x_{i+\frac{1}{2},j}(t) - H^x_{i-\frac{1}{2},j}(t)}{\Delta x} - \frac{H^y_{i,j+\frac{1}{2}}(t) - H^y_{i,j-\frac{1}{2}}(t)}{\Delta y} + S_{ij}(t) \tag{4}$$

The forth order 2D numerical fluxes, H^x and H^y are given below.

$$H^x_{i+\frac{1}{2},j} = \frac{a^+_{i+\frac{1}{2},j} F(U^E_{i,j}, B(x_{i+\frac{1}{2},j}, y_j)) - a^-_{i+\frac{1}{2},j} F(U^W_{i+1,j}, B(x_{i+\frac{1}{2},j}, y_j))}{a^+_{i+\frac{1}{2},j} - a^-_{i+\frac{1}{2},j}}$$

$$\frac{a^+_{i+\frac{1}{2},j} a^-_{i+\frac{1}{2},j}}{a^+_{i+\frac{1}{2},j} - a^-_{i+\frac{1}{2},j}} \left[U^W_{i+1,j} - U^E_{i,j}\right] \tag{5}$$

$$H^{y}_{i,j+\frac{1}{2}} = \frac{b^{+}_{i,j+\frac{1}{2}} G(U^{N}_{i,j}, B(x_i, y_{j+\frac{1}{2}})) - b^{-}_{i,j+\frac{1}{2}} G(U^{S}_{i,j+1}, B(x_j, y_{j+\frac{1}{2}}))}{b^{+}_{i+j+\frac{1}{2}} - b^{-}_{i+j+\frac{1}{2}}} \tag{6}$$

$$+ \frac{b^{+}_{i+j+\frac{1}{2}} b^{-}_{i+j+\frac{1}{2}}}{b^{+}_{i+j+\frac{1}{2}} - b^{-}_{i+j+\frac{1}{2}}} \left[U^{S}_{i,j+1} - U^{N}_{i,j}\right]$$

Where $a^{\pm}_{i\pm1/2,j\pm1/2}, b^{\pm}_{i\pm1/2,j\pm1/2}$ are the local one-sided speed of the propagation and are computed as follows:

$$a^{+}_{i+1/2,j} = \max\left\{ u^{E}_{i.j} + \sqrt{gh^{E}_{i,j}}, u^{W}_{i+1.j} + \sqrt{gh^{W}_{i+1,j}}, 0\right\}$$
$$a^{-}_{i+1/2,j} = \min\left\{ u^{E}_{i.j} - \sqrt{gh^{E}_{i,j}}, u^{W}_{i+1.j} - \sqrt{gh^{W}_{i+1,j}}, 0\right\}$$
$$b^{+}_{i+1/2,j} = \max\left\{ v^{N}_{i.j} + \sqrt{gh^{N}_{i,j}}, v^{S}_{i.j+1} + \sqrt{gh^{S}_{i,j+1}}, 0\right\}$$
$$b^{+}_{i+1/2,j} = \min\left\{ v^{N}_{i.j} - \sqrt{gh^{N}_{i,j}}, v^{S}_{i.j+1} - \sqrt{gh^{S}_{i,j+1}}, 0\right\}$$

$U^{E,W,N,S}$ are the point values of the piecewise linear reconstruction U = (*w, hu, hv*) for $\tilde{U}$ at location defined as $(x_{i+1/2,j}, y_{i,j}), (x_{i-1/2,j}, y_{i,j}), (x_{i,j}, y_{i,j+1/2}), (x_{i,j}, y_{i,j-1/2})$ .These point values are evaluated from a non-oscillatory piecewise polynomial reconstruction inside each grid cell from the cell averaged values of the variables *U(x,y).*

$$\tilde{U}(x,y) = \overline{U}_{ij} + (U_x)_{ij}(x - x_i) + (U_y)_{ij}(y - y_j) \qquad (x,y) \in C_{ij} \tag{7}$$

$\overline{U}$ is the mean value of the variables in the cell center. The numerical derivatives $(U_x)_{i,j}$ and $(U_y)_{i,j}$ are at least first-order component-wise approximations of $U_x(x_i, y_j, t)$ and $U_y(x_i, y_j, t)$. They are computed using a non-linear limiter function commonly known as minmod limiter.

$$(U_x)_{i,j} = \text{minmod}\left(\theta\frac{\overline{U}_{i,j} - \overline{U}_{i-1,j}}{\Delta x}, \frac{\overline{U}_{i+1,j} - \overline{U}_{i-1,j}}{2\Delta x}, \theta\frac{\overline{U}_{i+1,j} - \overline{U}_{i,j}}{\Delta x}\right), \tag{8}$$

$$(U_y)_{i,j} = \text{minmod}\left(\theta\frac{\overline{U}_{i,j} - \overline{U}_{i,j-1}}{\Delta y}, \frac{\overline{U}_{i,j+1} - \overline{U}_{i,j-1}}{2\Delta y}, \theta\frac{\overline{U}_{i,j+1} - \overline{U}_{i,j}}{\Delta y}\right), \tag{9}$$

The θ is a parameter for controlling numerical viscosity and for best result its value is taken as 1.3. The minmod function is defined as:

$$\text{minmod}\ (z_1, \ldots\ldots, z_n) = \begin{cases} \max\ z_i,\ z_i < 0\ \forall i, \\ \min\ z_i,\ z_i > 0\ \forall i, \\ 0, \quad otherwise \end{cases} \tag{10}$$

The function of this limiter is to construct the linear slope within each grid cell as a nonlinear

average of forward and the backward differences to prevent overshoots at the local maxima. The discretization of source terms is of crucial importance as the non-zero fluxes need to be balanced with the source terms in case of steady state solutions. The non-flux component of the flux terms in momentum equations is balanced with the source terms.

$$\left.\begin{aligned}\overline{S}_{i,j}^{(2)}(t) &\approx -g\frac{B(x_{i+\frac{1}{2}},y_j)-B(x_{i-\frac{1}{2}},y_j)}{\Delta x}.\frac{(w_{i,j}^{E}-B(x_{i+\frac{1}{2}},y_j))+(w_{i,j}^{W}-B(x_{i-\frac{1}{2}},y_j))}{2}\\ \overline{S}_{i,j}^{(3)}(t) &\approx -g\frac{B(x_i,y_{j+\frac{1}{2}})-B(x_i,y_{j-\frac{1}{2}})}{\Delta y}.\frac{(w_{i,j}^{N}-B(x_i,y_{j+\frac{1}{2}}))+(w_{i,j}^{S}-B(x_i,y_{j-\frac{1}{2}}))}{2}\end{aligned}\right\} \quad (11)$$

MODEL VALIDATION

Numerical Experiments

The numerical experiments were conducted to verify the accuracy of the model by simulating established benchmark test problems with the 1D version of the model. The initial conditions are taken from Zhou et al. (2001). Two selected tests cases are presented in this paper. One case is transcritical flow without a shock and another case is transcritical flow with a shock over a bump. The computational domain is constituted of 100 uniform cells of size Δx = 0.25m. The initial water depth of the whole domain is equal to the specified downstream flow depth of 0.4m and 0.33m respectively. The 1D bump in the 25m long channel was defined as follows:

$$B(x)=\begin{cases}0.02-0.05(x-10)^2 & \text{If } 8\text{m} < x < 12\text{m}\\ 0 & \text{otherwise}\end{cases}$$

Transcritical flow without a shock

A discharge per unit width of 1.53 m^2/s was imposed on the upstream boundary and downstream boundary conditions were open type. The Δt was computed from CFL criteria in all cases. The steady state reached after about 1500 iterations. The water surface elevation as a function of time at steady state is plotted in figure 3 which shows a very good agreement with the analytical solutions. The computed discharge is also compared with the theoretical as shown in figure 4.

Transcritical flow with a shock

A discharge per unit width of 1.18 m^2/s was imposed on the upstream boundary and 0.33m depth was imposed on the downstream boundary. The steady state reached after about 1800 iterations. It is shown in figure 6 that the computed water surface elevation at steady state shows a good agreement with the analytical solution. The computed discharge is also compared with the theoretical discharge as shown in figure 6.

Experimental comparison

The model is validated against the experimental data taken from Brufau et al. (2002). The experiments were conducted to generate a flood wave over a triangular bump resulting from a

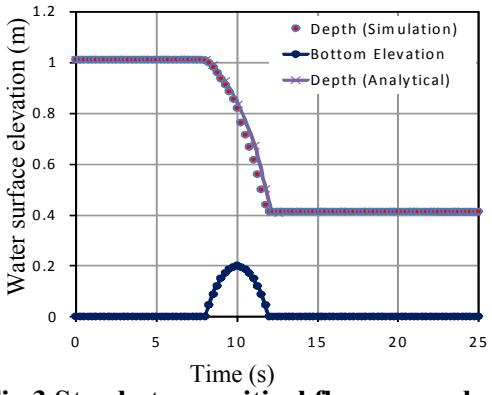

Fig.3 Steady transcritical flow over a bump without shock (Water surface).

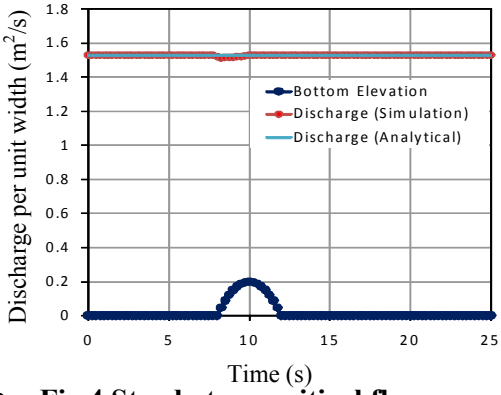

Fig.4 Steady transcritical flow over a bump without shock (Discharge).

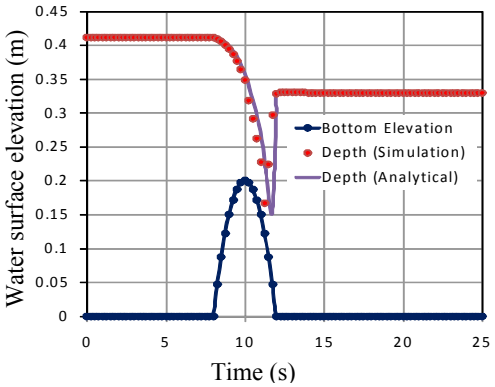

Fig.5 Steady transcritical flow over a bump with shock (Water surface).

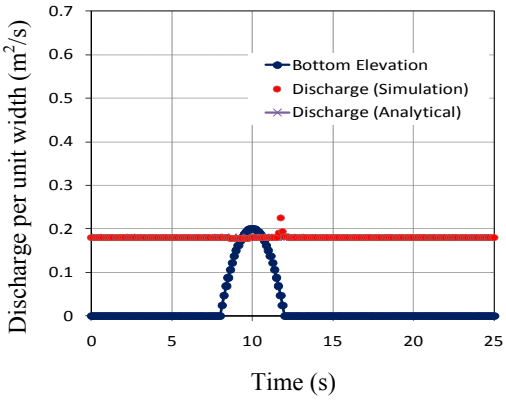

Fig.6 Steady transcritical flow over a bump with shock (Discharge).

dam failure. The schematic layout of the experiments is shown in figure 7**.** The experiments were conducted in a 38 meter long horizontal channel with a rectangular cross-section. The dam is located at 15.5m and the water depth in the reservoir upstream of the dam is 0.75m. A 6m long and 0.4m high triangular obstacle is located at 13m downstream of the dam. The channel is a fixed bed with dry initial conditions. The side boundaries are solid walls and the down-stream boundary conditions are open boundary type. The Δx is 0.01m and time step is computed by the CFL criteria. The Manning's coefficient n is 0.0125. The Gauge points (G) are located at 4 m, 10 m, 11 m, 13 m and 20 m downstream of the dam and are shown in figure 7.

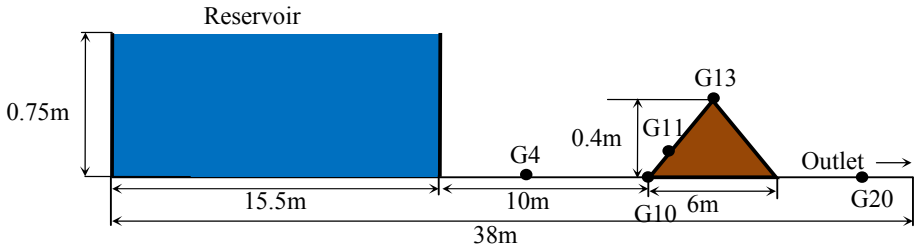

Fig.7 schematic diagram showing the experimental set up and observation points. (Brufau et al. 2002)

The predicted and measured water depths at 5 gauge points are plotted in figure 8 as a function of time. The flow regime changes from subcritical to transcritical and goes to supercritical flow at various gauge points during the course of time. The model reproduces the water depth at G4 to a good extent. At G10 and G11, the model slightly over-estimates the water depth at the beginning, however, after 15 seconds good agreement with the experiments is observed. The G13 is located at the tip of the triangular obstacle and is a critical point. The model slightly underestimates the maximum depth there. Nevertheless, the general trend is captured well despite a slight time lag. At G20, the trend is observed well and the water depth is slightly under-estimated. As a conclusion it can be said that the model predicts the water surface variations at various gauge points up to a reasonable good accuracy.

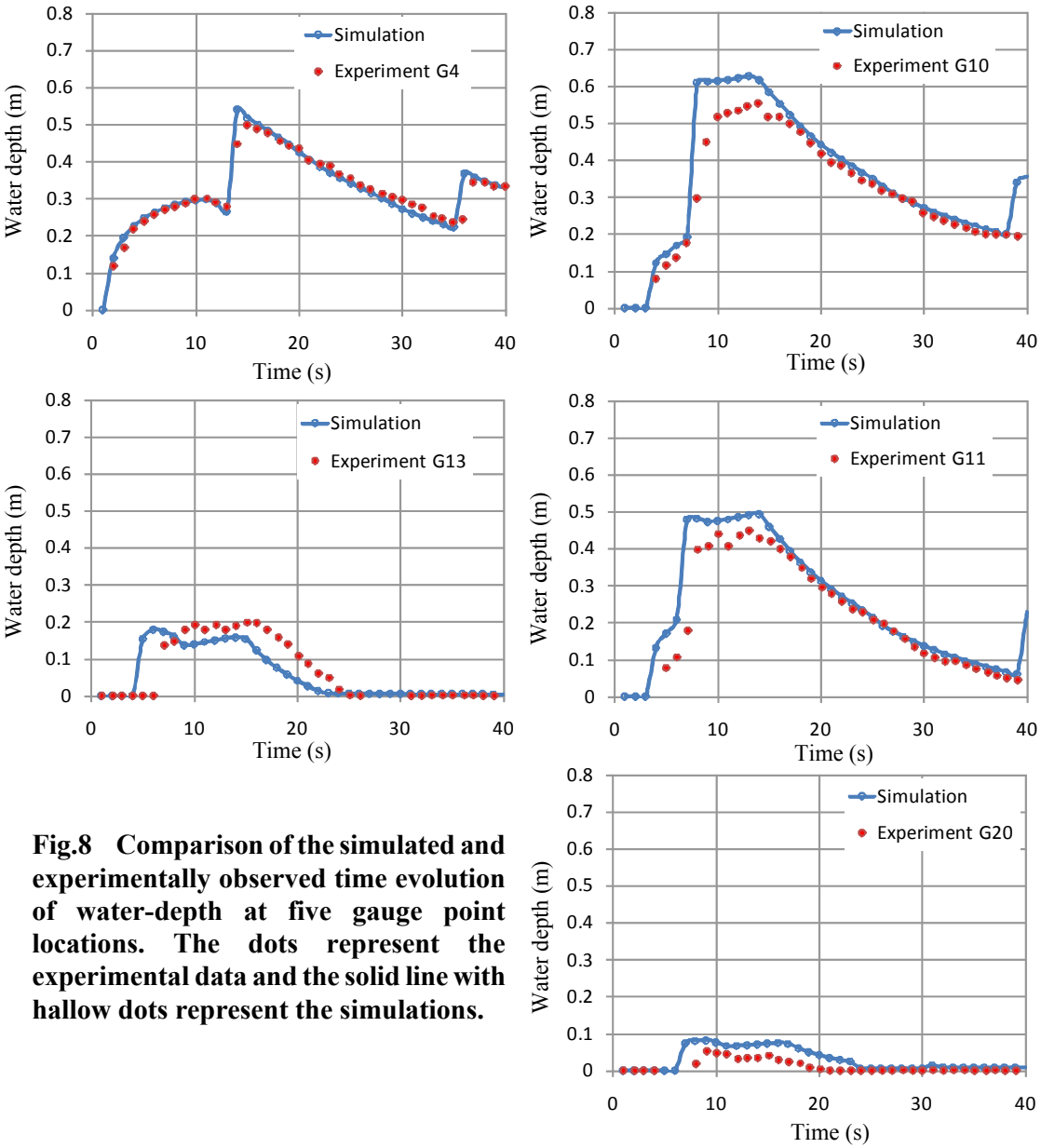

Fig.8 Comparison of the simulated and experimentally observed time evolution of water-depth at five gauge point locations. The dots represent the experimental data and the solid line with hallow dots represent the simulations.

MODEL APPLICATION

The two-dimensional version of this model was applied to simulate the historic Malpasset dam-break event that occurred on December 2, 1959, and resulted in a catastrophic flood that caused the death of 421 people in the downstream valley. Malpasset double-curvature arch dam was constructed on the Reyran River in France. The height of the dam was 66 meters and crest length was 223 meters. The maximum reservoir capacity was $55x10^6$ m^3. A physical model was built in 1962 to study the dam-break flow resulting from this catastrophic event. The front arrival times and the maximum water depths were measured at 9 observation points of the physical model. The location of the observation points and reservoir are shown in figure 9-A. The simulated water depth at 700 second and 2000 seconds after the dam failure is shown in figure 9-B and 9-C. It is observed that the model gives a realistic prediction of the flood depth at the downstream area. The flood arrival times computed at the observations points are compared with those observed from the physical model. The graph plotted in figure 10 shows that the flood front arrival time matches well with the observation data.

CONCLUSIONS

A two-dimensional numerical model is developed to numerically solve shallow water equations using Kurganov and Petrova (2007) scheme. This scheme is well balanced and preserves the positivity of the water depth at the discontinuous bottom surface. The simulation results from one-dimensional version of the model are compared with the analytical solutions of transcritical flow with and without a shock. The model reproduced the analytical solution results up to a very good accuracy. An experimental case of a dam break problem taken from the literature (Brufau et al. 2002) is simulated. It is shown that the flow depths computed at various gauge points agree with the experimental data. The two-dimensional version of the model was applied to simulate the real-life case of Malpasset dam break event. It is shown that the flood-arrival times computed at nine observation points of the physical model compare well with the observed data. The results of verification validation tests show that the model can be applied to simulate real-life dam-break flood flows.

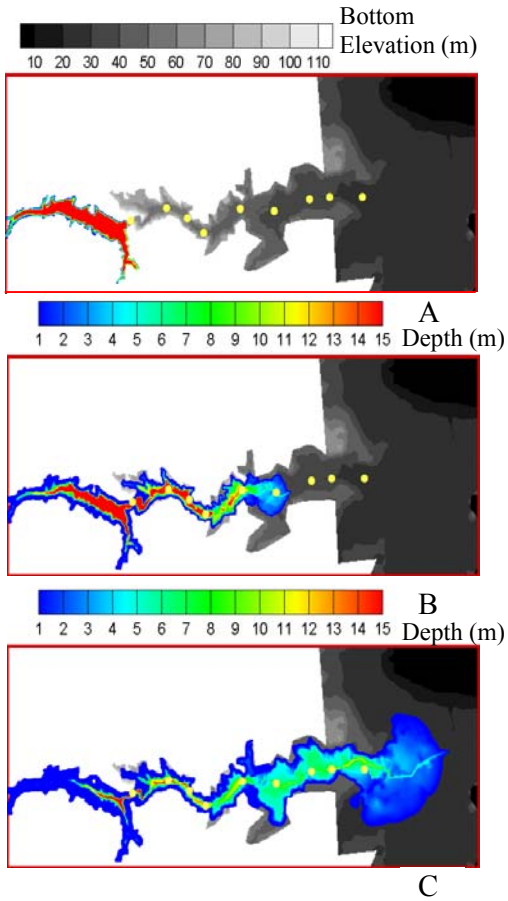

Fig.9 Location of observation points (yellow dots) and simulated water depth at 700s and 2000s from the failure of the Malpasset dam.

ACKNOWLEDGEMENTS

This research was funded by the Department of Homeland Security-sponsored Southeast Region Research Initiative (SERRI) at the Department of Energy's Oak Ridge National Laboratory, USA.

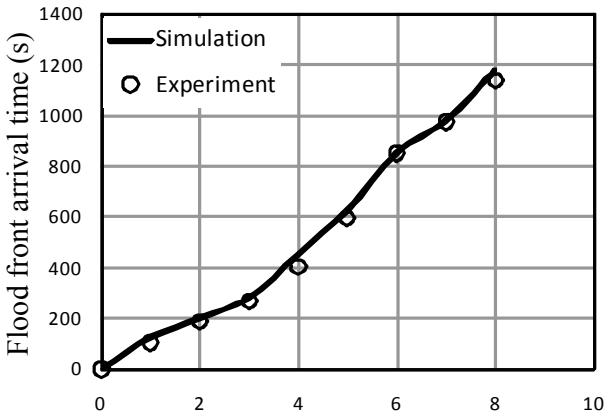

Fig.10 Comparison of simulated and observed flood front arrival time after the malpasset dam break event.

REFERENCES

Brufau, P., Vazquez-Cendon, M.E. and Garcia, P.N., 2002, A numerical model for flooding and drying of irregular domains, *International J. for Numerical Methods in Fluids,* 39, 247-275.

Brufau, P., Garcia, P.N., Vazquez-Cendon, M.E.,2004, Zero mass error using unsteady wetting-drying conditions in shallow flows over dry irregular topography, *International J. for Numerical Methods in Fluids,* 45,1047-1082.

Caleffi V., Valiani A, Zanni A., 2002**,** Finite volume method for simulating extreme flood events in natural channels. *J Hydraul Res.,* 41, 167-177.

Kurganov, A. and Levy, D. 2002, Central-Upwind scheme for Saint-Venant system, *M2AN Math. Model. Numer. Anal.,* 36, 397-425

Kurganov, A. and Petrova,G. 2007, A second order well balanced positivity preserving central upwind scheme for the saint- venant system, *Comm. Math. Sci.,* 5(1),133-160.

LeVeque, R.J. 1998, Balancing source terms and flux gradients in high resolution Godunov methods: the quasi-steady wave-propagation algorithm, *J. of Comp.Phys*, 146, 346-365.

Noelle, S., Pankratz,N., Puppo, G. and Natvig,J. 2006, well-balanced finite volume scheme for arbitrary order of accuracy for shallow water flows, *J. of Comp. Phys*, 213,474-499.

Russo,G. 2005, Central schemes for conservation laws with application to shallow water equations, Trends and application of mathematics to mechanics*, STAMM 2002*, S. Rionero and G. Romando (eds), 225-246, springer-verlag Italia SRL.

Valiani A, Caleffi V, Zanni,A., 2002, A. Case study,2002, Malpasset Dam-break simulation using two-dimensional finite volume method. *J. Hydraul Eng.,*128: 460-472.

Xinya Ying, Wang, S.Y.S, Khan, A.K.,2003, Numerical simulation of flood inundation due to dam and levee breech, Proceedings of *ASCE World Water and Environmental Resources Congress* , Philadelphia, USA.

Zhou, J.G., Causon, D.M., Mingham, C.G. and Ingram, D.M. 2001, Surface gradient method for treatment of source terms in the Shallow-Water Equations, *J. Comp. Phys*, 168, 1-25.